

# Thermal Dynamic Model and Analysis of Residential Buildings

Qiongyao Wang<sup>a</sup>, Tingjin Ren<sup>a</sup>, Yong Sun<sup>b</sup>, Yali Xue<sup>a,\*</sup>, Weiwei Fei<sup>c</sup>, Xinlei Wang<sup>d</sup>

<sup>a</sup>State Key Lab of Power Systems, Tsinghua University, Beijing, China

<sup>b</sup>State Grid Jilin Electric Power Company, Changchun, Jilin, China

<sup>c</sup>Changchun City Heating(Group) Co., LTD, Changchun, Jilin, China

<sup>d</sup>Beijing Huajian Wangyuan Power Design Institute, Beijing, China  
[xueyali@tsinghua.edu.cn](mailto:xueyali@tsinghua.edu.cn)

Northeast China has rich wind resources, while in the area where residential heating supply is mainly provided by combined heat and power (CHP) units, the curtailment of wind power is a serious problem in winter since the peak regulation capacity of CHP units is restricted by the demand for heat. The urban district heating (DH) system and residential buildings have huge heat storage capacities. To take full advantage of their heat storage capacity to improve the operational flexibility of CHP units, this paper explored the thermal dynamic of residential buildings. Basing on that, it explored the feasibility of regulating CHP units to increase the wind power integration. A first principle dynamic model of residential building was built in sub-station level of DH system, and then field test data of two districts in Changchun city were used to verify this model. The results showed that the model could simulate the dynamic of indoor temperature of buildings quite well when the heat supply and outdoor temperature changed. The influence of various heating supply scheduling modes on indoor temperature was finally compared basing on this model under typical outdoor temperature of winter. The results demonstrate the feasibility of future optimal scheduling of CHP units basing on thermal characteristics of residential buildings.

## 1. Introduction

Wind energy is a kind of clean and renewable energy. Increasing the use of wind energy can help reduce the consumption of fossil fuels and thus improve environmental quality. China has rich wind resources. According to the third survey of wind energy resources (CMA, 2009), the power generation capacity of China's onshore wind resources is equivalent to 22 Three Gorges Power Station in case of fully utilization. However, the abandonment of wind energy is very serious in China, especially in North China. For example, the annual utilization hour of wind power was only 1,333 h in Jilin Province, and the abandoned wind power ratio was up to 30 % (NEA, 2016). The main cause of this problem is that the urban heating supply of North China is mainly provided by combined heat and power (CHP) units, the power generation of which is severely restricted by the demand of heating, leaving little space for wind power integration. This has grown up to be a bottleneck for wind power utilization in China.

To enhance the wind power integration, the optimal scheduling of CHP units has gradually become a research hotspot based on heat storage technologies in recent years. The urban district heating (DH) system and buildings are existing built-up heat storage systems (Hu, 2016), owing to their good thermal insulation performance and high thermal inertia, so the thermal dynamic of them has gained much attention. While, compared with the transport delay of the heating network (Jie et al., 2012), the thermal dynamic of buildings is seldom introduced to the scheduling of heating supply. However, the performance of buildings is important in the optimization of heating supply scheduling (Ziemele et al., 2016).

Horvat and Dovic (2016) built a mathematical model to accurately predicting indoor temperature and space heating losses of a family, but the calculation load will increase dramatically when extended to a sub-station of the DH system, which has a large number of rooms and buildings. Sholahudin and Han (2016) built a simplified dynamic neural network model to predict the heating load of a building while the model precision depended much on the training data. A model identification approach was proposed (Harb et al., 2016) for forecasting the

building thermal response based on grey-box models, and four grey-box model structures were compared to find the best level of model complexity.

In this paper, a thermal dynamic model of residential building was built in sub-station level of DH system based on the first principle modelling, and then field test data was used for model verification. Based on this model, several heating supply modes were compared and the results demonstrated the feasibility of future optimal scheduling of CHP units basing on thermal dynamic of residential buildings.

## 2. Model and result

### 2.1 Model assumptions

Large-scale DH system usually includes a number of geographically dispersed heat-exchange stations or sub-stations. The heating area of each sub-station is different. The building insulation characteristics and the type of indoor radiators are not the same even in the same sub-station, so the detailed modelling of every room of the whole district will lead to large amounts of data collection and a huge computation load. But for the purpose of scheduling optimization algorithm, a light-weight model is more practical. In this paper, the thermal dynamic of all residential buildings of a sub-station are presented by a lumped parameter model. The heating load and outdoor temperature are defined as inputs, and indoor temperature is output. The short wave and long wave radiations are assumed to be known to calculate the outdoor colligate temperature.

### 2.2 Physical model

Ignoring the heat transfer process of less impact on indoor temperature, the physical model is set up. It comprises of six components and seven heat transfer processes. The six components include: water in radiator, radiator pipe, indoor air, interior wall, exterior wall base, thermal insulation layer of exterior wall. Every component has a lumped temperature. Assume that exterior wall is composed of exterior wall base and thermal insulation layer of exterior wall. The heat transferred through windows is considered into the thermal conductivity of the thermal insulation layer of exterior wall. The impact of radiation and environmental temperature is integrated into outdoor colligate temperature.

### 2.3 Mathematical model

According to the energy conservation principle and the heat transfer equation, formulas of water in radiator, radiator pipe, indoor air, interior wall, exterior wall base and thermal insulation layer of exterior wall can be established. The symbols and subscripts are defined in Table 1 and Table 2.

$$\frac{d(\rho_w V_{\text{pipe}} c_w T_w)}{d\tau} = W_{\text{we}} c_w T_{\text{we}} - W_{\text{wi}} c_w T_{\text{wi}} - Q_{\text{w2metal}} \quad (1)$$

$$Q_{\text{w2metal}} = h_{\text{w2metal}} A_{\text{metal\_inside}} (T_w - T_{\text{metal}}) \quad (2)$$

$$\frac{d(M_{\text{metal}} c_{\text{metal}} T_{\text{metal}})}{d\tau} = Q_{\text{w2metal}} - Q_{\text{metal2air}} \quad (3)$$

$$Q_{\text{metal2air}} = h_{\text{metal2air}} A_{\text{metal\_outside}} (T_{\text{metal}} - T_{\text{air}}) \quad (4)$$

$$\frac{d(M_{\text{air}} c_{\text{air}} T_{\text{air}})}{d\tau} = Q_{\text{metal2air}} - Q_{\text{air2stor}} - Q_{\text{air2split}} - Q_{\text{air2otsd}} \quad (5)$$

$$Q_{\text{air2stor}} = h_{\text{air2stor}} A_{\text{stor}} (T_{\text{air}} - T_{\text{stor}}) \quad (6)$$

$$Q_{\text{air2split}} = h_{\text{air2split}} A_{\text{split}} (T_{\text{air}} - T_{\text{split}}) \quad (7)$$

$$Q_{\text{air2otsd}} = \rho_{\text{air}} c_{\text{air}} V_{\text{in}} ACH (T_{\text{air}} - T_a) / 3600 \quad (8)$$

$$\frac{d(M_{\text{stor}} c_{\text{stor}} T_{\text{stor}})}{d\tau} = Q_{\text{air2stor}} \quad (9)$$

$$\frac{d(M_{\text{split}} c_{\text{split}} T_{\text{split}})}{d\tau} = Q_{\text{air2split}} - Q_{\text{split2shell}} \quad (10)$$

$$Q_{\text{split2shell}} = \lambda_{\text{shell}} A_{\text{shell}} \frac{T_{\text{split}} - T_{\text{shell}}}{\Delta_{\text{shell}}} \quad (11)$$

$$\frac{d(M_{\text{shell}} c_{\text{shell}} T_{\text{shell}})}{d\tau} = Q_{\text{split2shell}} - Q_{\text{shell2otsd}} \quad (12)$$

$$Q_{\text{shell2otsd}} = h_{\text{shell2otsd}} A_{\text{shell}} (T_{\text{shell}} - T_z) \quad (13)$$

$$T_z = T_a + Q_{\text{irrad}} \frac{a_f}{\alpha_A} \quad (14)$$

Geometrical parameters of buildings are found in Thermal Design Code for Civil Buildings (MCPRC, 1993) and Annual Report on China Building Energy Efficiency (BERC, 2013). Parameters of radiator are set according to the product information. The physical parameters at room temperature are taken as the calculation parameters.

Table 1: Variables

Symbol	Meaning	Unit	Symbol	Meaning	Unit
$A$	area	$\text{m}^2$	$V$	volume	$\text{m}^3$
$M$	mass	kg	$W$	mass flow rate	kg/s
$\rho$	density	$\text{kg}/\text{m}^3$	$c$	specific heat capacity	$\text{J}/(\text{kg}\cdot\text{K})$
$\Delta$	thickness	m	$d\tau$	time step	s
$Q$	heat flux	W	$T$	temperature	$^{\circ}\text{C}$
$\lambda$	heat conductivity coefficient	$\text{W}/(\text{m}\cdot\text{K})$	$T_z$	outdoor colligate temperature	$^{\circ}\text{C}$
$V_{\text{pipe}}$	volume of water in radiator	$\text{m}^3$	$ACH$	air change rate	-
$h$	convective heat transfer coefficient	$\text{W}/(\text{m}^2\cdot\text{K})$	$a_f$	absorption coefficient of thermal insulation of exterior wall	-
$\alpha_A$	convective heat transfer coefficient between outdoor air and thermal insulation layer of exterior wall	$\text{W}/(\text{m}^2\cdot\text{K})$			

Table 2: Subscripts

Symbol	meaning	symbol	meaning
w	water in radiator	stor	interior wall
we	inlet of radiator	a	outdoor air
wl	outlet of radiator	split	exterior wall base
metal	radiator pipe	shell	thermal insulation layer of exterior wall
air	indoor air	w2metal	between water in radiator and radiator pipe

## 2.4 Model validation

The field data of two districts in Changchun are used for model validation. The relative error of indoor temperature between the calculated result and measured data is less than 7.6 % shown in Figure 1 and Figure 2. For a long period of one week, the calculated indoor temperature fits the measured data quite well, see Figure 3. RE means relative error.

## 2.5 Model simplification

Taking Anda district as an example, the characteristics of the residential building model are analysed and simplified, which will also be used in section 3. When heating load drops 10 % from 9.46 MW to 8.51 MW and outdoor colligate temperature maintains  $-5^{\circ}\text{C}$ , the identified transfer function between heating load and indoor air temperature is obtained, as shown in Eq(15):

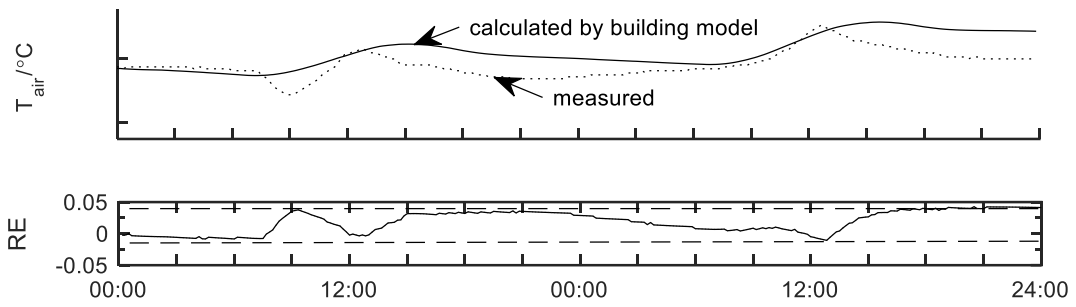


Figure 1: Indoor temperature and relative error of Anda district during 11-12 March, 2016

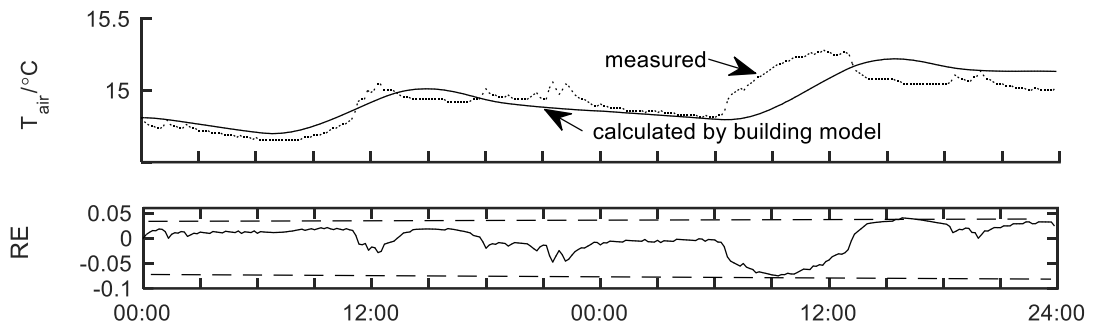


Figure 2: Indoor temperature and relative error of Xinyi district during 13-14 March, 2016

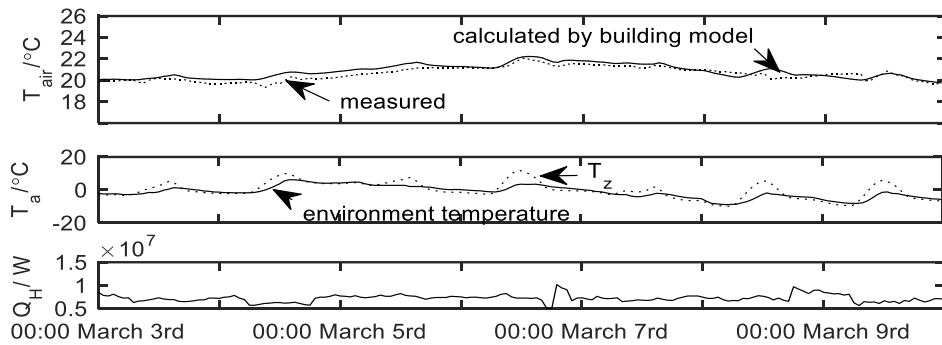


Figure 3: Indoor temperature, heating load and outdoor temperature of Anda district during 3-10 March, 2016

$$\frac{T_{air}(s)}{Q_H(s)} = \frac{0.0001615s + 3.153 \times 10^{-9}}{s^2 + 0.0001539s + 2.524 \times 10^{-9}} \quad (15)$$

When outdoor colligate temperature drops from -5 °C to -10 °C, and heating load maintains 9.46 MW, the identified transfer function between outdoor colligate temperature and indoor air temperature is obtained, as shown in Eq(16). To sum up, the identified model is shown in Eq(17).

$$\frac{T_{air}(s)}{T_z(s)} = \frac{2.992 \times 10^{-5}}{s + 0.0001213} \quad (16)$$

$$T_{air}(s) = \frac{0.0001615s + 3.153 \times 10^{-9}}{s^2 + 0.0001539s + 2.524 \times 10^{-9}} Q_H(s) + \frac{2.992 \times 10^{-5}}{s + 0.0001213} T_z(s) \quad (17)$$

The results calculated by the theoretical model and identified model almost coincide, so the identified model can replace the theoretical model. This reduces model complexity and saves computing time.

### 3. Discussion

#### 3.1 Impact of inputs

Using the measured heating load during 00:00 am, March 3rd to 00:00 pm, March 10th, 2016 and the average outdoor colligate temperature during this period as input data to calculate the indoor temperature. As it can be observed in Figure 4(a), the effect of heating load on indoor temperature is to maintain the indoor temperature at a certain level. Using outdoor colligate temperature and the average heating load during this period as input data to calculate the indoor temperature, the effect of outdoor colligate temperature on indoor temperature is periodic, as it can be observed in Figure 4(b).

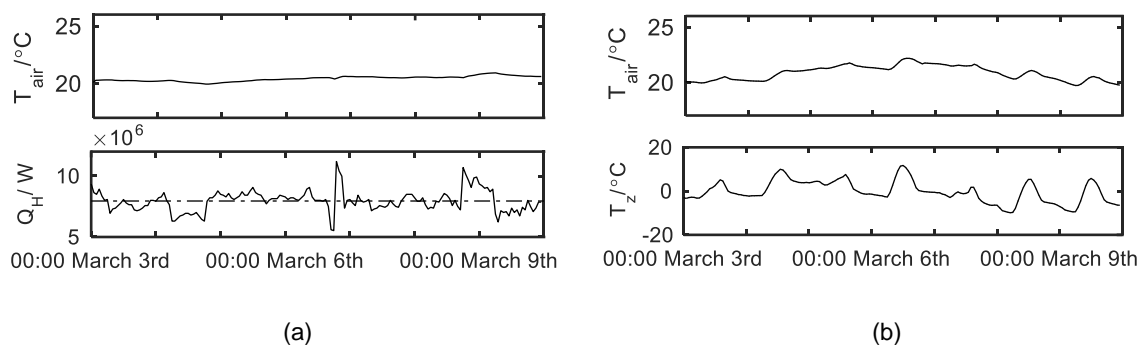


Figure 4: Impact of input: (a) heating load change (b) outdoor colligate temperature change

#### 3.2 Heating supply modes

Here several heating supply modes are compared to demonstrate the impact of heat scheduling on indoor temperature. Take the outdoor temperature and heating load as input data (during 20:00 pm, 19 December - 20:00 pm, 20 December, 2016) to calculate the indoor temperature. Three modes are studied:

- Mode 1: heating load maintains 40 W/m<sup>2</sup> all day.
- Mode 2: heating load decreases to 20 W/m<sup>2</sup> during 00:00 am to 12:00 am, then increases to 60 W/m<sup>2</sup> during 13:00 pm to 24:00 pm, while the mean heating load remains 40 W/m<sup>2</sup> every day.
- Mode 3: heating load decreases to zero during 00:00 am to 6:00 am, then increases to 40 W/m<sup>2</sup> during 7:00 am to 12:00 am, increases to 120 W/m<sup>2</sup> during 13:00 pm to 18:00 pm, and decreases to zero during 19:00 pm to 24:00 pm; the mean heating load remains 40 W/m<sup>2</sup> every day.

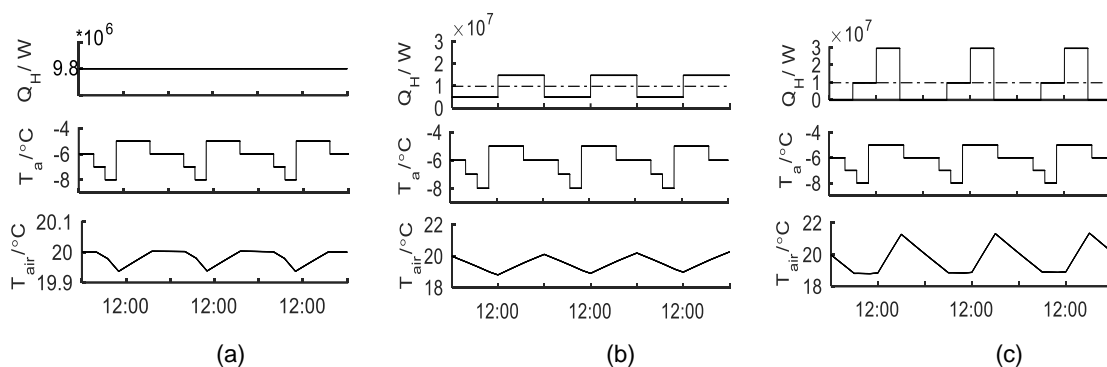


Figure 5: Indoor temperature under various heating supply modes: (a) Mode 1 (b) mode 2 (c) mode 3

Assume the outdoor temperature changes periodically, and then calculate indoor temperature consecutively for three days. The curve of indoor temperature, outdoor temperature and heating load are shown in Figure 5. The indoor temperature is compared in Table 3. From Figure 5 and Table 3, it shows that:

1) When the mean daily heating load remains the same, all three heating supply modes could meet the heat demand with indoor temperature always above 18 °C. Under continuous and stable heating mode (mode 1),

average indoor temperature is the highest and the fluctuation is slight. Under intermittent heating mode (mode 2 and mode 3), average indoor temperature is lower and the fluctuation is violent.

2) Mode 2 and mode 3 could all help increase peak regulation capacity of CHP units. At the period of lower heating load, the CHP unit has a wider range of power regulation, and more wind power could be integrated into the grid by reducing the power generation of CHP units. The price paid is the fluctuation of the indoor temperature.

*Table 3: Comparison of different heating modes*

Heating mode	1	2	3
minimum indoor temperature (°C)	19.94	18.8	18.8
maximum indoor temperature (°C)	20	20.27	21.36
range of indoor temperature (°C)	0.06	1.47	2.56
standard deviation of indoor temperature (°C)	0.02	0.38	0.82
average indoor temperature (°C)	19.98	19.53	19.78

In the premise of ensuring heating supply, the thermal dynamic model proposed in this paper could predict the indoor temperature under given outdoor temperature as well as the heating load curve. This makes it possible to optimize the heating and power load dispatching of CHP units when wind power prediction information is available.

#### 4. Conclusions

This paper established a thermal dynamic model of residential building and field test data were used for model verification. The results show that the model could simulate the dynamic of indoor temperature of residential buildings quite well when the heat supply and outdoor temperature changed.

The impact of outdoor temperature and heating load is analysed based on some field data, then the influence of several heating supply modes on indoor temperature is compared basing on the proposed model under typical outdoor temperature of deep winter. The results show that, by reducing the heat load at some suitable period, the peak regulation capacity of CHP units can be improved in the blowout period of wind power generation and this makes it possible to integrate more wind power into the grid. The model proposed in this paper provides the thermal dynamic of residential buildings, which is the basis for optimal heat and power load dispatching of CHP units to improve wind power utilization.

#### Acknowledgments

The work is supported by National Key Technology R&D Program (No.2015BAA01B01), and the authors gratefully acknowledge the financial support from State Grid Corporation of China.

#### References

- Building Energy Research Centre (BERC), Tsinghua University, 2013. Annual Report on China Building Energy Efficiency, China Construction Industry Press, Beijing, China, 294 ps. ISBN: 978-7-112-15260-5.
- China Meteorological Administration (CMA), 2009. China Wind Energy Resource Assessment, China Meteorological Press, Beijing, China, 142 ps. ISBN: 978-7-5029-4989-1.
- Harb H., Boyanov N., Hernandez L., Streblov R., Müller D., 2016, Development and Validation of Grey-box Models for Forecasting the Thermal Response of Occupied Buildings, *Energy and Buildings*, 117, 199-207.
- Horvat I., Dovic D., 2016, Dynamic Modelling Approach for Determining Buildings Technical System Energy Performance, *Energy Conversion and Management*, 125, 154-165.
- Hu Y.L., 2016, Analysis on Thermal Performance of Composite Wall of Energy-saving Buildings, *Chemical Engineering Transactions*, 51, 1183-1188.
- Jie P.F., Tian Z., Yuan S.S., Zhu N., 2012, Modeling the Dynamic Characteristics of a District Heating Network, *Energy*, 39, 126-134.
- Ministry of Construction of the People's Republic of China (MCPRC), 1993, Thermal Design Code for Civil Buildings, China Planning Press, Beijing, China, 125 ps. ISBN: 978-15-80058-23-0.
- National Energy Administration (NEA), 2016. Wind Power Integration in 2016, <[www.nea.gov.cn/2017-01/26/c\\_136014615.htm](http://www.nea.gov.cn/2017-01/26/c_136014615.htm)>, accessed 23.02.2017.
- Sholahudin S., Han H., 2016, Simplified Dynamic Neural Network Model to Predict Heating Load of a Building Using Taguchi method, *Energy*, 115, 1672-1678.
- Ziemele J., Pakere I., Chernovska L., Blumberga D., 2016, Lowering Temperature Regime in District Heating Network for Existing Building Stock, *Chemical Engineering Transactions*, 52, 709-714.